Does G_0 of Granular Materials Carry Information on Their Particle Characteristics?

B. N. Madhusudhan and M. C. Todisco

Abstract Small strain elastic properties, such as G_0, are used to model the soil behaviour under dynamic and static loading. In granular materials, these depend mainly on effective stress and density. However, the influence of particle morphology on G_0 cannot be neglected. This paper presents series of laboratory experiments on different granular materials using resonant column apparatus and bender elements. The combined effect of particle morphology, size and distribution of glass ballotini and quartz sands was investigated by using micro-mechanics based analytical model. Experimental results indicate that the A and n parameters of the $G_0 = A^*f(e)^*(p'/p_r)^n$ relationship are linked to particle size, roughness and shape. Using an analytical model, A and n parameter is expressed as function of particle characteristics. The potential use of G_0 to predict particle characteristics is explored in this study.

Keywords Stiffness · Particle roughness · Quartz sand · Glass ballotini · Analytical model

1 Introduction

Small strain elastic properties are essential to describe behaviour of granular materials under static and dynamic loading for problems ranging from granular flows to earthquake. The shear modulus (G_0) is a fundamental material property used in modelling of uncemented granular soils, which is generally expressed as function of density and effective stress using equation 1 [1–3]. Much research has demonstrated that A and n are material parameters that can be related to effective stress and density/state [1, 4, 5]. On the other hand particle characteristics such as

B. N. Madhusudhan (✉) · M. C. Todisco
University of Southampton, Southampton, UK

Coffey Geotechnics, Manchester, UK
e-mail: M.Bangalore-Narasimha-Murthy@soton.ac.uk

P. Giovine et al. (eds.), *Micro to MACRO Mathematical Modelling in Soil Mechanics*, Trends in Mathematics, https://doi.org/10.1007/978-3-319-99474-1_24

particle size, distribution [2, 6, 7] and morphology [4] also influence small strain material properties. However, G_0 relation to particle characteristics is not well established [2, 7, 8].

$$G_0 = A_G F(e)\left(\frac{p^/}{p_r}\right)^{n_G} \tag{1}$$

The macro-mechanical behaviour of granular materials depends on packing structure and particle contact behaviour. Analytical and numerical studies on small strain elastic properties have identified the link between micro and macro response of granular materials at particle level due to particle arrangement and particle contact distribution within the assembly along with particle rearrangement due to change in stress condition [9–12]. This paper explores the role of particle characteristics such as grain size, shape and roughness on small strain shear modulus of glass ballotini and a quartz sand through experimental and numerical analysis. For simplicity, G_0 in this study refers to small strain shear modulus in the vertical direction (G_{vh}).

2 Granular Materials and Small Strain Stiffness Testing

In order to examine the effect of particle characteristics on small strain shear modulus, uniform spherical glass ballotini and sub-angular sand particles of similar size (d_{50}) along with a poorly graded particle size distribution were chosen for the comparative study (Table 1). The sand is the Cauvery River sand from Karnataka, India, which is naturally well-graded consisting of 80% quartz, 18% feldspar and 2% mica. Figure 1 shows the grading curves of the uniform sands and the medium graded sand. Particle characteristics such as sphericity and roundness of sands was characterised by using SEM images of sands as given in Fig. 2 and the Krumbein and Sloss chart [13]. 3D roughness of granular materials was characterised to obtain an average RMS (Root Mean Square) of the asperity heights using an interferometer. The RMS roughness, S_q, was obtained over a field of view (scan area) of approximately 40 × 40 μm, which was kept constant for each particle type and size (Fig. 3). This allowed to compare S_q values, the roughness being sensitive to the scan area. A scan area of 141.5 × 106 μm was also used. While for glass ballotini, the undetected points were less than 1% also for large scan areas, i.e. reliability of roughness values, for some sand grains the undetected points were larger than 1%. A field of view of 40 × 40 μm was selected based on an acceptable percentage of undetected points (<1%) and the fact that inter-particle contact areas would be less than 40 × 40 μm [14, 15]. The contact radius was also obtained from interferometer measurements.

Cylindrical granular assemblies were prepared and tested at different isotropic effective stress (25–500 kPa) for small strain elastic properties using resonant column apparatus with bender/extender element inserts [6]. The granular assemblies were prepared in two different packing densities, poured random packing (PRP) and closed random packing (CRP), by using a dry pluviation method as described in

Table 1 Granular material index and particle characteristics used in the study

Granular material	Packing	Void ratio (e)	Average Roughness Sq[a] (μm)	Roundness[b]	Sphericity[b]	A_G	n_G
Glass ballotini 2 mm	CRP	0.65	0.099	1	1	318.9	0.502
	PRP	0.69				151.7	0.450
Glass ballotini 0.6 mm	CRP	0.63	–	1	1	218.1	0.540
	PRP	0.71				132.1	0.513
Glass ballotini 0.3 mm	CRP	0.65	–	1	1	197.4	0.616
	PRP	0.73				120.5	0.546
Coarse sand $d_{50} = 2.5$ mm	PRP	0.75	0.431–0.526	0.3	0.9	76.4	0.480
	CRP	0.61				75.7	0.470
Medium sand $d_{50} = 0.60$ mm	PRP	0.76	0.347	0.4	0.8	73.0	0.470
	CRP	0.62				71.4	0.440
Fine sand $d_{50} = 0.30$ mm	PRP	0.78	–	0.4	0.8	68.0	0.502
	CRP	0.64				70.3	0.478
Medium-fine sand	PRP	0.74	–	0.4	0.7	63.2	0.452
	CRP	0.56				83.6	0.341

[a]Average of 10 tests each on 40 × 40 μm field of view
[b]Roundness and Sphericity obtained from Kumbrein and Sloss chart [20]

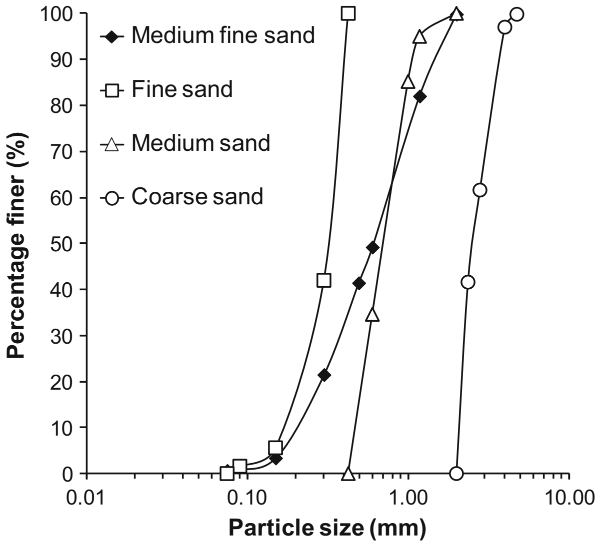

Fig. 1 Particle size distributions of Cauvery River sand used for the study

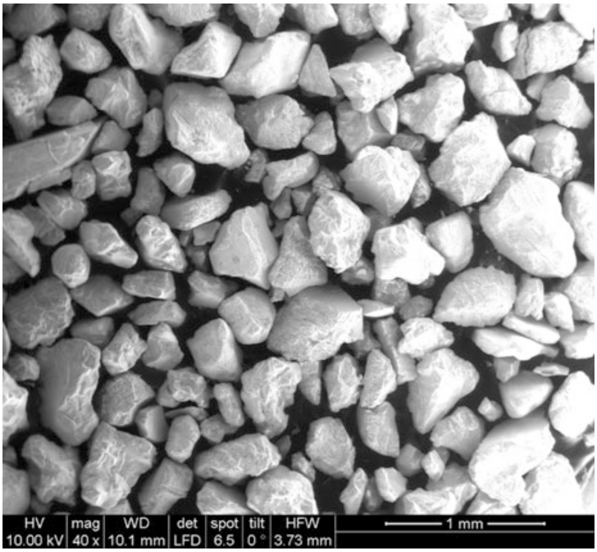

Fig. 2 Example of SEM image of medium sand used for particle characterisation

Kumar & Madhusudhan [6]. PRP was achieved by pouring the granular materials from zero height of fall, while CRP was achieved by pouring the granular material from calibrated height of fall using a pluviation device [16]. The index properties, void ratio and particle characteristics of granular materials used are presented in Table 1.

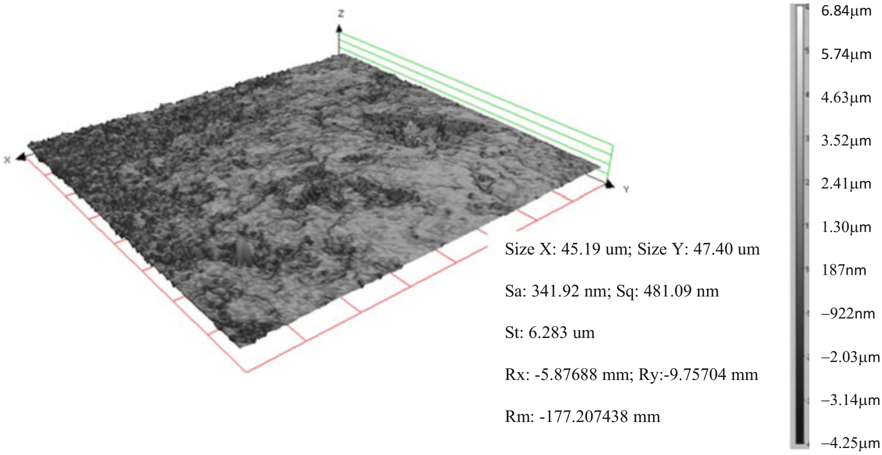

Fig. 3 Typical 3D view of Cauvery river sand (coarse) surface evaluated using interferometer

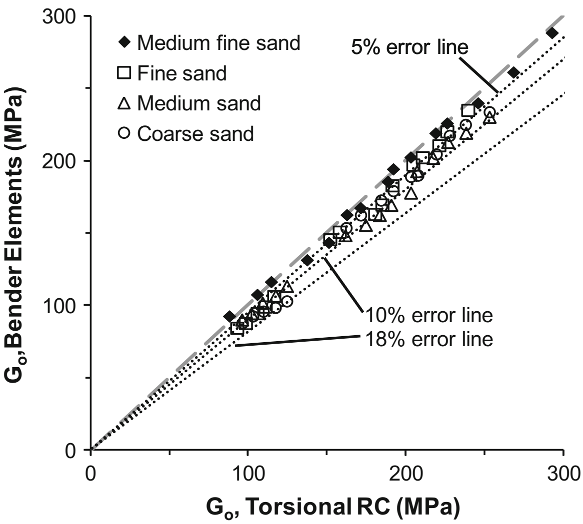

Fig. 4 Comparison of G_0 obtained from resonant column and bender element tests

Small strain shear modulus (G_0) was calculated from the sample resonant frequency at different isotropic stresses obtained for small torsional vibrations applied at top of the sample, fixed at the bottom (torsional vibration of a cantilever beam) in the resonant column device. Details regarding resonant column testing can be found in Madhusudhan & Senetakis [16, 17]. Shear wave pulse was transmitted from the top and received at the bottom of the specimen using bender elements to compare the two methods of obtaining G_0 [6, 16]. Figure 4 presents the comparison of the two methods of obtaining shear modulus. In general, there is a good agreement between the resonant column and bender element test results. Error lines indicate that the average scatter for the uniform sands is 10%. Only two data points show maximum error of 18% for the coarse sand at low effective stresses (100 kPa). This discrepancy may be due to coupling between the particles and the elements in the BE tests.

3 Effect of Particle Characteristics on G_0

Experimental results from the testing programme designed to capture the effect of particle size, shape with respect to density and effective stress is presented in Fig. 5. Spherical shaped glass beads of 2, 0.6 and 0.3 mm diameter can be compared with their corresponding sub-angular coarse, medium and fine sands of similar d_{50} particle size. G_0 increases with increase in effective stress and density of assembly regardless of particle shape and size, however the increase in magnitude is affected by the particle characteristics, which is discussed in next section.

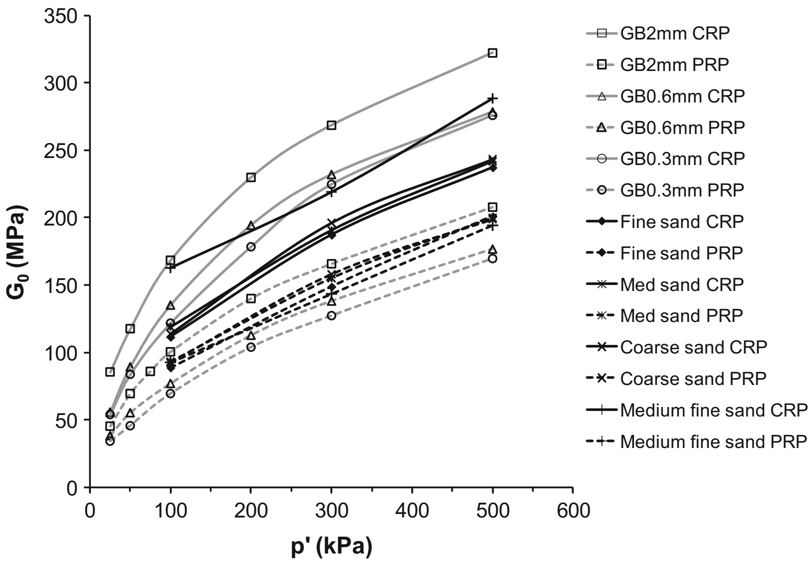

Fig. 5 Effect of particle size and shape on G_0

3.1 Effect of Particle Size and Morphology

The effect of particle size on G_0 is more evident in the spherical glass ballotini than in the sub-angular sand particles. The material parameters A_G and n_G were derived for each test by normalising G_0 with F(e) and p' with p_{ref} in Eq. (1), where void ratio function F(e) was taken as $e^{1.3}$ and p_{ref} as atmospheric pressure as referred in Senatakis & Madhusudhan [17]. Table 1 presents the material parameters: both A_G and n_G derived for spherical particles are larger than those for sub-angular. The A_G decreases with decreasing particle size and packing density while n_G increases. This trend is more evident in the spherical particles.

3.2 Effect of Grading

Table 1 shows that the A_G and n_G parameters are sensitive to the type of grading. The medium graded sand mixture shows larger A_G and lower n_G values than the uniform sands. This is mainly attributed to the packing density as a medium graded mixture allows reaching denser packing, therefore higher coordination number.

4 Comparison with Numerical Models

The G_0 values measured by bender elements and resonant column testing are compared with values calculated by micro-macro mechanics analytical models for rough-surface contacts [9, 11, 18]. The calculation was carried out for both glass ballotini and Cauvery River sand particles of 2 mm and d_{50} of 2.50 mm, respectively, but only results for the sand are shown and commented.

4.1 Analytical Procedure

In the rough-surface contact model [11, 13], the contact stiffnesses depend on the particle roughness. Experimental data have shown that roughness at the particle contact might change due the applied load and displacement. Senetakis et al. [15] found a reduction in roughness of 33% for a pair of quartz sand particles subjected to normal and tangential inter-particle forces ranging between 0.5 and 5 N. In this work, roughness values were assumed to be constant with increasing isotropic effective stress. The calculated contact forces experienced by particles subjected to a maximum isotropic effective stress of 500 kPa were smaller than those experienced in the recent micro-mechanical testing [e.g. 14, 15]; therefore, the assumption of unique roughness value throughout the test is justified. In the case of Cauvery river sand with d_{50} of 2.50 mm, an average of S_q between large and medium particles was adopted, i.e. $S_q = 0.478\ \mu m$.

In this calculation, the particle dimension that is involved in the formulation of the micro-macro mechanics rough-surface contact model has been taken as the radius of curvature of the assumed contact area. Shi and Polycarpou [19] adopted a rough-surface contact model assuming that the particle dimension involved in the contact mechanism was the radius of the asperities which were considered spherical. In this paper, the roughness was measured over an area of approximately $40 \times 40\ \mu m$, therefore it was assumed that the radius of the contact area was equivalent the radius of curvature of the scan area. The calculation follows the static hypothesis approach for which the contact forces in any direction can be calculated as [10]:

$$f_i = \frac{\sigma_i \left(r^2\right) 4\pi\ (1 + e)}{Cn} \tag{2}$$

where σ_i is the stress acting on the assembly, r is the radius of curvature of the contact area obtained from interferometry testing, e is the void ratio of the assembly and C_n is the coordination number calculated as 13.28-8e [10].

The rough micro-mechanical contact model introduces the rough contact area a_r as a function of the α parameter and the Hertzian contact area, a. The parameter relates the roughness to the Hertzian deformation of the particle δ_0, the normal contact force, the particle dimension (radius of curvature of the contact area in the present study) and particle shear modulus. Yimsiri and Soga [11] presented a hyperbolic expression for the relationship a_r and α to fit the data provided in [13]. This relationship was used to calculated a_r. The deformation at the particle contact was calculated by substituting the rough contact area, a_r, to Hertz contact area, a.

The normal contact stiffness K_n was calculated as the secant between two consecutive increments of normal contact forces, derived from the macroscopic isotropic stress. For example, $K_{n,100\text{–}300}$ represents the normal stiffness between 100 and 300 kPa isotropic stress and can be calculated as:

$$K_{n,100-300} = \frac{\Delta f}{\Delta \delta} = \frac{f_{300} - f_{100}}{\delta_{300} - \delta_{100}} \tag{3}$$

The K_n values are used to calculate the shear modulus in the middle of the isotropic stress interval. This was a practical choice to relate the macroscopic stress changes to the microscopic contact forces. The tangential stiffness was considered as a ratio of the normal contact stiffness calculated for smooth contact [18]. It was assumed that particles at the contact have already mobilised the inter-particle friction angle, φ_r, i.e. tangential forces in the horizontal plane are equal to $f_n \tan \varphi_r$.

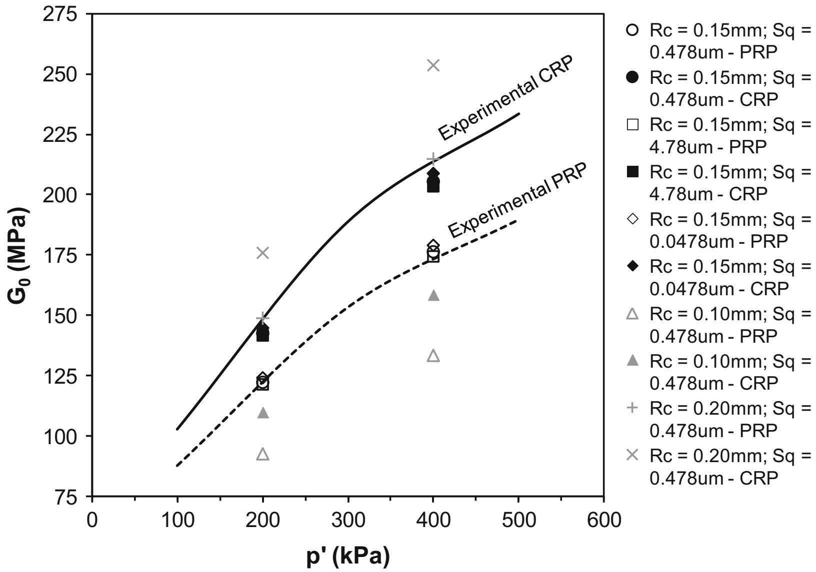

Fig. 6 Comparison of G_0 from experiments and rough surface analytical model for natural sand

4.2 Results

Figure 6 compares the macroscopic shear modulus of the Cauvery river sand obtained from experimental testing and analytical models. The G_0 approximate better the experimental data by increasing/reducing only roughness, while it agree worse if contact areas are reduced/increased. The material parameters A_G and n_G for the coarse sand from the analysis ($Rc = 0.15$; $S_q = 0.478$) was 171.41 and 0.52 for CRP, whereas 116.16 and 0.51 for PRP. The model is successful in capturing the state and effective stress dependency of G_0 and also the decreasing trend of A_G and n_G, but due to lack of sufficient input data of void ratio and effective stress the absolute values do not match with those shown in Table 1. Although the macroscopic isotropic stress intervals are large, the G_0 from the rough contact model and the experimental data agree well. A parametrical study was carried to investigate the effect of roughness and magnitude of contact area (Rc) on the G_0.

5 Conclusions

This work presents experimental and numerical study on the influence of particle characteristics on shear modulus (G_0). The experiment results show the effect of particle size is dominant for spherical shaped particles of low surface roughness, whereas it is subtle for sub-angular rough surface grains. The material parameters are sensitive to the shape of the grading curves as a mixed grading allows creating denser packing. However, this aspect is being investigated. Micro-mechanics based analytical model successfully captured the effect of state and effective stress on G_0 incorporating surface roughness and shape and size of the contact area. Experimental and initial numerical results indicate that the A and n parameters of the $G_0 = A^*f(e)^*(p'/p_r)^n$ relationship are linked to particle size, roughness and shape. From the parametric study, surface roughness (S_q) seems to less significant role compared to contact radius (Rc). Using the analytical model, stiffness 'n' parameter can be expressed as function of coordination number and particle morphology. Thus G_0 can be potentially used to predict particle characteristics but further studies on particle characteristics such as particle surface contact area are required.

Acknowledgments We acknowledge Indian Institute of Science, Bangalore, India, Faculty of Engineering and the Environment of the University of Southampton and Department of Civil Engg., The University of Hong Kong for providing the facilities to carry out the experimental work.

References

1. Hardin, B., Drnevich, V.: Shear modulus and damping in soils: measurement and parameter effects. J. Soil Mech. Found. ASCE. **18**(SM6), 603–624 (1972)
2. Wichtmann, T., Triantafyllidis, T.: On the influence of the grain size distribution curve of quartz sand on the small strain shear modulus G_{max}. J. Geotech. Geoenviron. Eng. ASCE. **135**(10), 1404–1418 (2009)
3. Kumar, J., Madhusudhan, B.N.: Dynamic properties of sand from dry to fully saturated states. Geotechnique. **62**(1), 45–55 (2012)
4. Hardin, B.O., Richart, F.E.: Elastic wave velocities in granular soils. J. Soil Mech. Found. Div., Proc. ASCE. **89**(SM1), 33–65 (1963)
5. Jovičić, V., Coop, M.R.: Stiffness of coarse-grained soils at small strains. Geotechnique. **47**(3), 545–561 (1997)
6. Kumar, J., Madhusudhan, B.N.: Effect of relative density and confining pressure on Poisson ratio from bender and extender elements. Geotechnique. **60**(7), 630–634 (2010)
7. Yang, J., Gu, X.Q.: Shear stiffness of granular material at small strains: does it depend on grain size? Geotechnique. **63**(2), 165–179 (2013)
8. Menq, F.Y., Stokoe, K.H.: Linear dynamic properties of sandy and gravelly soils from large-scale resonant tests. In: Di Benedetto, H., Geoffroy, H., Doanh, T., Sauzeat, C. (eds.) Deformation characteristics of geomaterials, pp. 63–71. Swets & Zeitlinger, Lisse, the Netherlands (2003)
9. Goddard, J.D.: Nonlinear elasticity and pressure-dependent wave speeds in granular media. Proc. R. Soc. Math. Phys. Sci. **430**(1878), 105–131 (1990)
10. Chang, C.S., Misra, A., Sundaram, S.S.: Properties of granular packings under low amplitude cyclic loading. Soil Dyn. Earthq. Eng. **10**(4), 201–211 (1991)
11. Yimsiri, S., Soga, K.: Micromechanics-based stress-strain behaviour of soils at small strains. Geotechnique. **50**, 559–571 (2000)
12. Otsubo, M., O'Sullivan, C., Hanley, K., Sim, W.: The influence of particle surface roughness on elastic stiffness and dynamic response. Géotechnique. **67**(5), 452–459 (2016)
13. Greenwood, J.A., Tripp, J.H.: The elastic contact of rough spheres. J. Appl. Mech. (ASME). **34**, 153–159 (1967)

14. Senetakis, K., Coop, M., Todisco, M.C.: The inter-particle coefficient of friction at the contacts of Leighton Buzzard sand quartz minerals. Soils Found. **53**(5), 746–755 (2013)
15. Senetakis, K., Coop, M.R., Todisco, M.C.: Tangential load-deflection behaviour at the contacts of soil particles. Géotech. Lett. **3**(2), 59–66 (2013)
16. Madhusudhan, B.N., Senetakis, K.: Evaluating use of resonant column in flexural mode for dynamic characterization of Bangalore sand. Soils Found. **56**(3), 574–580 (2016)
17. Senetakis, K., Madhusudhan, B.N.: Dynamics of potential fill–backfill material at very small strains. Soils Found. **55**(5), 1196–1210 (2015)
18. Mindlin, R.D.: Compliance of elastic bodies in contact. J. Appl. Mech. **16**, 259 (1949)
19. Shi, X., Polycarpou, A.A.: Measurement and modeling of normal contact stiffness and contact damping at the meso scale. J. Vib. Acoust. **127**, 52–60 (2005)
20. Krumbein, W.C., Sloss, L.L.: Stratigraphy and sedimentation, 2nd edn. Freeman, San Francisco (1963)